Pyroxene relations in two Hawaiian hypersthene-bearing basalts

By I. D. Muir and J. V. P. Long

Department of Mineralogy and Petrology, Cambridge

Summary. A preliminary account is given of an optical and electron-microprobe investigation into the pyroxene relations of Hawaiian hypersthene-bearing lavas. It is shown that the clinopyroxene jackets to the phenocryst hypersthenes consist of strongly zoned augite, not pigeonite as formerly believed; the compositional range of this pyroxene is approximately the same as that of the groundmass augite phase. Groundmass pyroxene relations are complex; in one case two distinct pyroxene phases, augite and pigeonite occur, in the other all compositions lying between augite and pigeonite are encountered.

Introduction

HAWAIIAN tholeiitic basalts display two main types of pyroxene assemblage: those that contain a single clinopyroxene phase and those that contain orthopyroxene as well. The former may be typified by the lavas of Kilauea; these frequently contain phenocrysts of magnesian augite with subcalcic augite in the groundmass; more differentiated types carry subcalcic augite alone. The lavas of Mauna Loa, on the other hand, commonly have slender microphenocrysts of hypersthene, typically mantled by a narrow sheath of highly birefringent clinopyroxene believed to be pigeonite. Many of these lavas also contain small microphenocrysts of augite. The groundmass of this type is always exceedingly fine-grained and is composed of groups of tiny overlapping granules of clinopyroxenes that appear to range from a nearly uniaxial pigeonite to 'pigeonitic augite' with $2V$ up to 35°. Some grains appear to grade continuously from one to the other, whilst in other cases in the same rock, the two appear to be sharply defined. The same relations hold for the basalts of the Koolau series of Oahu, except that hypersthene more frequently appears as a true phenocryst, and in many cases microphenocrysts of augite are lacking. Similar relations have been described by Kuno (1955) from Japanese lavas.

A number of hypersthene-bearing Hawaiian lavas have been studied by Muir and Tilley (1963) who reported analyses of two hypersthenes, and two associated groundmass clinopyroxene fractions. It was shown

that the hypersthenes varied somewhat in composition and showed distinct enrichment in iron towards the margins. Owing to the small initial sample size and separation difficulties it was not possible to obtain samples sufficient for chemical analysis that were completely free from clinopyroxene contamination and this is reflected in the high lime content (6·65 %) of the Mauna Loa analysis. In the Koolau sample removal of the augite grains from the analysed fraction also led to the removal of most of the lighter hypersthene phenocryst material and the analysis therefore represents the bulk composition of the microphenocryst hypersthene with a small amount of contamination from the occasional microphenocrysts of pigeonite. From this study, it was not possible to establish whether there was any variation in the lime content of the orthopyroxene with change in the iron magnesia ratio, or whether the jacketing clinopyroxene, believed to have crystallized after eruption, differed significantly in composition from that of the groundmass.

The two analyses given of the groundmass pyroxenes from these rocks showed significantly lower lime contents than those of the Kilauean type; in agreement with Kuno's results their plotted positions in the pyroxene system lay on the orthopyroxene side of the postulated pyroxene cotectic curve. These analyses were considered to represent the bulk composition of the dominant pyroxene of the groundmass, referred to as 'pigeonitic augite', but which could also be regarded as a very lime rich member of the pigeonite series. Both fractions were known to be contaminated slightly by fragments derived from augite microphenocrysts and by a little of the groundmass pigeonite.

In order to investigate further the pyroxene relations in this type of basalt an optical and electron-microprobe study has been made of two chemically similar analysed rocks which display best the jacketing of the hypersthene. One of these, 68211, comes from the Koolau series (analysis Muir and Tilley, *op. cit.*, table 1, no. 6), the other, 66084, is a specimen from the 1868 lava of Mauna Loa (analysis Muir and Tilley, table 5*a*, no. 5).

Electron-probe analyses

The concentration of calcium and iron in individual grains has been determined by electron-probe analysis on two polished thin sections. X-ray intensities were referred to standards of pure iron and wollastonite. In the instrument used for the measurements the electron beam is incident normally on the surface of the specimen and X-rays are collected at an angle of 40° to the surface. All measurements were made

with a beam accelerating voltage of 20 kV and at probe currents in the range 6×10^{-8} A and 2×10^{-7} A. Under these conditions the resolution in silicates is of the order of 2 μ.

The small grain size and the presence of closely intergrown ore grains created difficulties in the analysis of groundmass material owing to the possibility of minerals overlapping within the volume excited by the probe. In order to determine the pattern of zoning in the clinopyroxene jackets to the hypersthene the probe was traversed in approximately 1 μ steps, first for the determination of calcium, and then for iron. The current in the probe is stable to better than 1 % for periods of half an hour so that no reference to standards is necessary during such runs. On the other hand, since it is difficult to reproduce exactly the position of the probe to better than about 0·5 μ in the successive runs, the correlation of the calcium and iron traverses becomes unreliable in the presence of inclusions and steep concentration gradients. For this reason determinations have also been made by resetting the spectrometer from Fe$K\alpha$ to Ca$K\alpha$ with the probe stationary on one point in the jacket. The sequence of measurements is then: Fe (metal)–Fe (jacket)–Ca (jacket)–Ca (wollastonite). All measurements on the groundmass pyroxenes and on microphenocrysts have been made in the same way. Since the microprobe is equipped with only one spectrometer, it was not possible to extend this procedure to the simultaneous measurement of magnesium, and this element has therefore been estimated by difference. The minor constituents have not been determined and in calculating the pyroxene formulae the scaling factors already used for the chemical data (Muir and Tilley, 1963, table 2, analyses 6 and 6′) have been employed for the Koolau results. The Mauna Loa analyses of clinopyroxenes have been scaled on the basis of the chemical analysis no. 4 but in view of the known contamination of the fraction 4′, the scaling factor obtained from analysis 6′ has been used for the hypersthenes. The trend of the microphenocryst compositions along a line of constant iron rather than constant magnesium, which shows most clearly in the Koolau results, may in part be due to increase in the content of the minor components in the clinopyroxene of the groundmass as revealed by analyses of successive Kilauean pyroxene fractions.

Statistical fluctuations in the numbers of recorded quanta are such as to give a probable error not greater than ±2 % of the listed values, and usually not more than ±1 % in the case of the iron determinations. (All measurements are the result of at least two determinations, each

taking 10 seconds, during which time the recorded count is $\sim$ 2000/1 % FeO.)

The measurements have been corrected for the normal instrumental factors of resolving time and background count rate and also for the effects of absorption, fluorescence excitation (Ca$K\alpha$ by FeK) and differences in mean atomic number of the standards and unknowns. The factors by which the X-ray intensity ratios have been multiplied are shown in table I.

TABLE I. Correction factors for determination of Fe and Ca with standards of pure iron and wollastonite

Take-off angle = 40°. Beam accelerating voltage 20 kV

	Hypersthenes		Pigeonites		Augites	
	Fe	Ca	Fe	Ca	Fe	Ca
Absorption	0·999	1·036	1·000	1·032	1·006	1·024
Fluorescence	—	0·999	—	0·998	—	0·999
Atomic number	1·14	1·00	1·14	1·00	1·12	1·00

The largest correction is for the atomic-number effect in the iron determinations; these were estimated using a procedure developed by Reed (1964), which has been shown experimentally to give accurate compensation, at least over the atomic number range Z = 8–30. No attempt has been made to correct for fluorescence excitation of Ca$K\alpha$ by FeK in the neighbourhood of phase boundaries. In the extreme case of hypersthene in contact with augite, the increase in the measured calcium content of the hypersthene within 2 μ of the boundary will be less than 0·1 % CaO.

In measurements which include the simultaneous estimation of magnesium together with iron and calcium, the optimum beam accelerating voltage would be appreciably lower than the 20 kV used here. A compromise between the requirements of reducing the absorption of Mg$K\alpha$ and maintaining a reasonable over-voltage for Fe$K\alpha$ would suggest a value of about 15 kV.

Hypersthene basalt 68211, Koolau Series, Oahu

Hypersthene occurs as two generations, both as stout scattered phenocrysts up to 3 mm in length, many of which are jacketed by clinopyroxene and much more abundantly as zoned microphenocrysts up to $\frac{1}{2}$ mm in length which occur mostly as clusters of four or five grains, associated with microphenocrysts of augite, and very occasionally of pigeonite. The orthopyroxene microphenocrysts are less commonly

TABLE II. Electron-probe analyses of pyroxenes from basalt 68211, Koolau series, Oahu

Description	FeO	CaO	Adopted composition Wo	(En)*	Fs
Core of jacketed hypersthene	9·4	2·0	4·1	78·8	17·0
Jacketing augite					
1*a*	8·9	19·1	41·0	43·8	15·2
1*b*	9·1	16·1	34·6	49·8	15·6
1*c*	10·2	17·5	37·6	44·9	17·5
1*d*	12·6	18·0	38·8	39·7	21·5
1*e*	11·5	15·7	33·8	46·5	19·7
1*f*	10·1	17·0	36·6	46·1	17·3
1*g*	9·5	16·3	35·0	48·7	16·3
Augite microphenocrysts					
1*a*	7·1	17·9	38·5	49·3	12·2
1*b*	6·5	18·3	39·4	49·5	11·1
1*c*	6·8	17·0	36·6	51·8	11·6
1*d*	7·6	15·9	34·2	52·8	13·0
1*e*	7·7	15·0	32·2	54·6	13·2
1*f*	6·9	18·3	39·4	48·8	11·8
Groundmass augites					
1	10·5	18·3	39·4	42·6	18·0
2	8·3	18·3	39·4	46·4	14·2
3	9·6	16·6	35·7	47·9	16·4
4	8·6	15·2	32·7	52·6	14·7
5	6·8	17·6	37·8	50·5	11·7
6	8·4	17·1	36·8	48·8	14·4
7	10·5	15·9	34·2	47·8	18·0
8	11·4	17·4	37·5	43·0	19·5
9 (intergrown grain)	7·3	17·8	38·3	49·2	12·5
pigeonites					
1 (intergrown grain)	14·7	4·5	9·0	67·8	23·2
2	14·8	4·6	9·2	67·4	23·4
3	13·6	3·7	7·4	71·1	21·5
4 (adjacent to iddingsite)	15·2	3·9	7·8	68·2	24·0

* By difference.

jacketed and their jackets are narrower. The microprobe investigation has shown that the phenocrysts are distinctly more magnesian than the microphenocrysts, FeO values rising from 9·4 % in the core to 10·1 % at the margin in the example studied. The lime content on the other hand appears to increase only slightly towards the margin (table II, analyses 1 and 2).

Pigeonite. Rare microphenocrysts of magnesian pigeonite ($\gamma = 1{\cdot}723$, $2V = 6°–10°$, optic plane $\perp$ (010) occur with the orthopyroxene microphenocrysts and clearly crystallized along with them across the

inversion interval; a similar occurrence has been described by Kuno and Nagashima (1952). The composition of this pigeonite has not yet been determined.

The investigation of a typical augite microphenocryst reveals a range of compositions already suggested by the observed variation in $2V$;

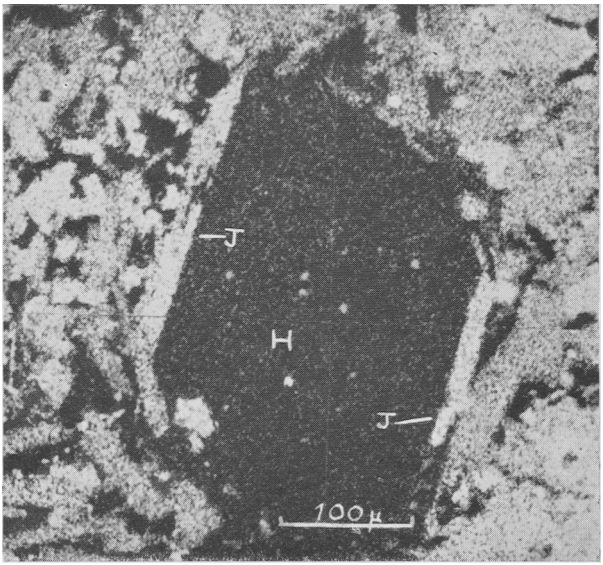

FIG. 1. X-ray scanning picture taken with Ca$K\alpha$ radiation (white areas are calcium rich) showing a large hypersthene phenocryst (H), with its clinopyroxene jacket (J).

this crystal is zoned from augite $Ca_{39\cdot4}Mg_{49\cdot5}Fe_{11\cdot1}$ towards subcalcic augite $Ca_{32\cdot2}Mg_{54\cdot6}Fe_{13\cdot2}$ with some oscillatory zoning. The pyroxene appears to remain magnesia rich; like the Kilauean augite microphenocrysts it is distinctly more magnesian than the optical properties would indicate, presumably due to a relatively high content of chromium and titanium. These microphenocrysts are notably more magnesian than the jacketing pyroxene and appear to have crystallized in equilibrium with the orthopyroxene and pigeonite microphenocrysts.

The jackets range from 10 μ to 20 μ in width but they are discontinuous and are mainly confined to the prism faces of the orthopyroxene as shown in fig. 1. In some cases, however, the two pyroxenes are intergrown and the clinopyroxene may form a central lamella embedded in the orthopyroxene (Muir and Tilley, plate I, fig. 3). They display very

complex zoning involving changes in Mg, Fe, and Ca as shown by a typical trace across a jacket (fig. 2).

In general lime reaches its highest value (19 %) in the very narrow zone immediately adjacent to the orthopyroxene. The associated small

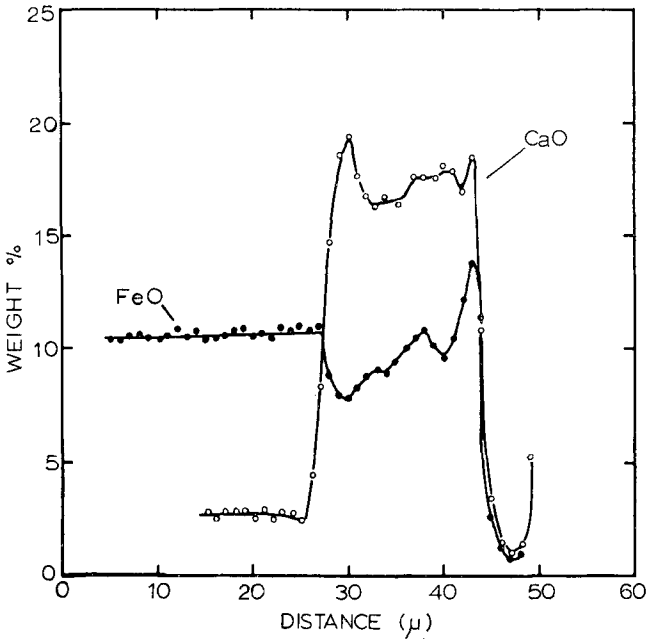

FIG. 2. Distribution of iron and calcium in the outer region of a hypersthene phenocryst and in the surrounding clinopyroxene jacket.

decrease in this constituent observed in the outermost parts of the orthopyroxene suggests that a post-crystallization exchange of calcium occurred as the contiguous pyroxenes became adjusted to their solvi. A similar effect in adjacent clinopyroxene lamellae has been recorded by Binns, Long, and Reed (1963, fig. 2).

Except for this contact effect a lime content of about 16 % is constantly observed in the inner part of the jacket, and this increases generally to reach about 18 % at the margin, usually with one or more oscillations. Iron also increases very steeply in the extreme margins; that this is a genuine feature of the pyroxene and not just an effect produced by a narrow layer of iron oxide along the outer boundary has

been confirmed by a traverse for silicon. Optically, under very high magnification the extreme margins display a significantly deeper colour accompanied by a marked increase in refractive index. The intermediate values of lime and iron displayed in the traverse (fig. 2) across the orthopyroxene–clinopyroxene boundary appear to be caused by a fracture aligned along the junction plane which is vertical.

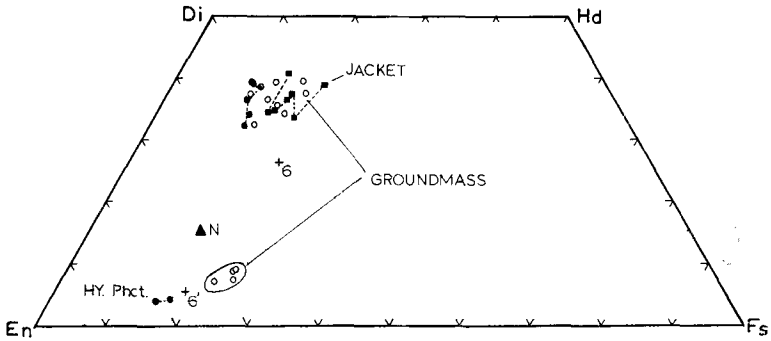

FIG. 3. Compositions (mol. % $CaSiO_3$, $MgSiO_3$, $FeSiO_3$) of individual pyroxene grains from the Koolau basalt as determined by electron-probe analysis for calcium and iron, magnesium being estimated by difference assuming minor element contents as given by bulk chemical analysis. ● Microphenocryst, ○ groundmass; dashed lines connect measurements made on zoned grains. 6, 6′ compositions of groundmass clinopyroxene and microphenocryst hypersthene respectively, determined by chemical analysis; ▲ *N* normative pyroxene of rock (mol. %).

From fig. 3 it can be seen that except for the innermost zone of the jacket whose composition is believed to have changed, the range of compositions encountered in the jacketing pyroxene is the same as that of the groundmass augite.

Groundmass pyroxenes. Here two distinct pyroxenes occur, a subcalcic augite sometimes zoned and forming crystals up to 80 μ in diameter, and a pigeonite; random sampling for lime content made over approximately 100 grains indicated that the majority were of subcalcic augite (ratio of about 4:1), but that they were sometimes intergrown with pigeonite in a complex fashion. From this ratio and a survey of the plotted pyroxene compositions as shown in fig. 4 it is clear that the analysed composition (point 6), accurately reflects the bulk composition of the groundmass pyroxene of this rock. Two of these intergrown grains are shown in the scanning pictures for iron (figs. 4*a* and 4*b*). The presence of the two phases in parallel crystallographic orientation in

these composites and the effect of overlapping layers of contrasted composition is clearly responsible for the wide range of $2V$ values previously recorded. In the grains figured the y-axis is nearly vertical and this has prevented an accurate determination of the range of $2V$ values of the two phases. Indirect measurements, however, suggest that the range of $2V$ in the augite phase is between 45° and 35° and that the pigeonite remains essentially uniaxial.

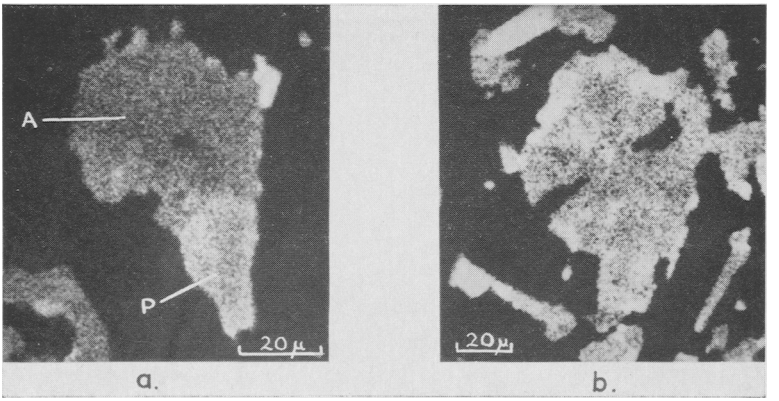

FIG. 4. Koolau basalt. X-ray scanning pictures taken with Fe-$K\alpha$ radiation (white areas iron rich). (*a*) Composite grain of groundmass pyroxene composed of zoned subcalcic augite (*A*) and zoned pigeonite (*P*). Bright grain on top right corner of pyroxene is magnetite. (*b*) A more complex example of a composite groundmass grain composed of zoned subcalcic augite with intergrown areas of pigeonite. The merging boundary near left top corner of the grain is caused by pigeonite inclined at a low angle to the surface.

Around the large phenocrysts of olivine (Fa_{16}) with iddingsite rims there are well-developed coronas of granular pyroxene; the probe investigation has revealed that this pyroxene consists entirely of pigeonite whose composition, FeO 15·2, CaO 3·9 is slightly more iron-rich and calcium-poor than the typical pigeonite of the groundmass. Augite makes its appearance only at a distance of some 50–100 μ from the olivine margin; here it has a lime content of just over 18 % and it immediately becomes the more abundant pyroxene. It would appear therefore that the composition gradient due to the reaction of olivine is confined to the immediate neighbourhood defined by the reaction corona.

TABLE III. Electron-probe analyses of pyroxenes from basalt 66084, Mauna Loa, Hawaii

Description	FeO	CaO	Wo	(En)*	Fs
Hypersthenes: core of jacketed phenocryst	9·7	2·6	5·2	79·5	15·3
cores of unjacketed microphenocrysts					
1	9·9	2·8	5·6	78·7	15·7
2	8·9	2·3	4·6	81·3	14·1
3	10·5	2·8	5·6	77·8	16·6
4	10·4	2·4	4·8	78·8	16·4
5	9·6	2·6	5·2	79·6	15·2
6	10·4	3·2	6·4	77·2	16·4
Augite microphenocrysts					
1	8·2	17·4	41·0	43·7	15·3
2	7·5	17·5	41·2	44·8	14·0
3*a*	7·5	18·1	42·6	43·4	14·0
3*b*	7·5	17·1	40·4	45·6	14·0
3*c*	6·7	18·8	44·4	43·1	12·5
3*d*	9·5	14·3	33·7	48·5	17·8
4*a*	7·0	18·4	43·4	43·5	13·1
4*b*	7·8	16·1	38·0	47·4	14·6
4*c*	6·9	18·1	42·6	44·5	12·9
4*d*	6·9	16·9	39·8	47·3	12·9
Groundmass pyroxene					
1	14·6	9·0	21·2	51·5	27·3
2	9·7	15·9	37·5	44·4	18·1
3	11·4	11·1	26·2	52·8	21·0
4	15·0	6·6	15·6	56·4	28·0
5	7·5	17·5	41·3	44·7	14·0
6	15·6	11·3	26·6	44·2	29·2
7	14·3	7·6	17·9	55·3	26·8
8	11·4	10·9	25·7	53·3	21·0
8*a*	12·6	12·8	30·2	46·2	23·6
9	9·7	12·9	30·4	51·5	18·1
9*a*	7·3	17·1	40·3	46·0	13·7
10	11·1	16·1	38·0	41·3	20·7
11	15·7	14·6	29·4	35·7	29·4

Hypersthene basalt 66084, 1868 lava of Mauna Loa

This rock carries large phenocrysts of olivine (Fa_{13}) with very much less obvious coronas of granular pyroxene, an occasional phenocryst of hypersthene Of_{15} and abundant zoned microphenocrysts of the same mineral Of_{16-20}, typically with clinopyroxene jackets. The jacketing pyroxene is sometimes intergrown with the orthopyroxene in a complex manner. Large microphenocrysts of augite also occur. The groundmass is extremely dense and fine grained (average size 5–10 μ) but its pyroxene

appeared to range from pigeonite to pigeonitic augite with $2V \simeq 30°$, values between these extremes occurring in different grains with individual grains showing some range of zoning (up to 10°) in the rare cases where reliable measurements of the optic angle could be made.

X-ray microanalysis, the results of which are plotted in fig. 5, has revealed that the hypersthenes are more lime-rich than in the Koolau

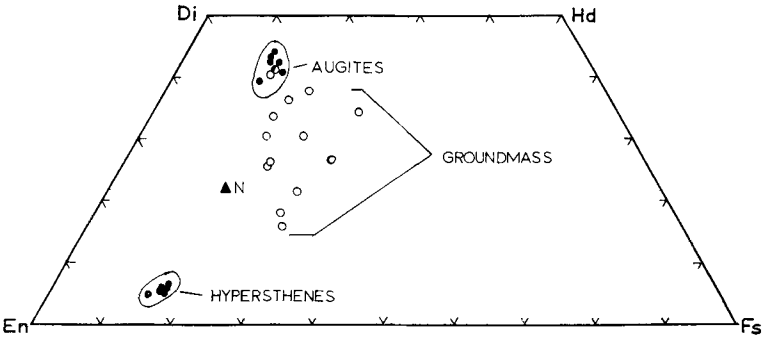

FIG. 5. Compositions (mol. % $CaSiO_3$, $MgSiO_3$, $FeSiO_3$) of individual pyroxene grains from the Mauna Loa basalt as determined by electron-probe analysis. ● Microphenocrysts, ○ groundmass; ▲ *N* normative pyroxene of rock (mol. %).

rock and that they are distinctly more magnesian than the optical properties indicated, suggesting an analogy with the hypersthene of the Uwekahuna Gabbro (Muir and Tilley, 1957, p. 249). As in the Koolau basalt the microphenocrysts of augite are more magnesian than the optical properties suggest and display complex oscillatory zoning due presumably to pressure changes before eruption. The jacketing pyroxene appears to be an augite with complex zoning, but because of its discontinuous nature it was not possible to make accurate measurements of the different zones. The groundmass pyroxenes reveal a considerable scatter and cover the whole range from subcalcic augite to lime rich pigeonite. It is significant that normal pigeonite compositions were not encountered in the body of the rock; pigeonite may occur as a local reaction product with the olivine but it was not possible to obtain measurements on this pyroxene because of its small grain size.

Discussion

The results obtained from these specimens indicate that the lime content of the orthopyroxene tends to increase slightly with iron enrichment during crystallization and that the microphenocrysts of this

mineral crystallized in equilibrium with the augite microphenocrysts before the lava was erupted. The jacketing pyroxene appears to be merely a parallel growth effect that commenced under intratelluric conditions, possibly just before eruption, and was completed under extrusive conditions. In the Koolau lava the pyroxene solvus has clearly been effective in determining the nature and compositions of the groundmass phases which show remarkably little scatter in composition as zoning and different times for nucleation are involved.

The Mauna Loa basalt clearly crystallized under somewhat different conditions, for its hypersthenes are more lime rich and its microphenocryst augites on average more lime poor than in the Koolau rock. The pyroxene solvus has not been effective in controlling the compositions of the groundmass pyroxenes, which are scattered over a wide field.

References

Binns (R. A.), Long (J. V. P.), and Reed (S. J. B.), 1963. Nature, vol. 198, p. 777.
Kuno (H.), 1955. Amer. Min., vol. 40, p. 70.
—— and Nagashima (K.), 1952. *Ibid.*, vol. 37, p. 1000.
Muir (I. D.) and Tilley (C. E.), 1957. Amer. Journ. Sci., vol. 255, p. 241.
—— —— 1963. *Ibid.*, vol. 261, p. 111.
Reed (S. J. B.), 1964. Ph.D. dissertation, University of Cambridge.